
On the Bottleneck of Graph Neural Networks and its Practical Implications

Uri Alon
Technion

urialon@cs.technion.ac.il

Eran Yahav
Technion

yahave@cs.technion.ac.il

Abstract

Graph neural networks (GNNs) were shown to effectively learn from highly structured data containing elements (nodes) with relationships (edges) between them. GNN variants differ in how each node in the graph absorbs the information flowing from its neighbor nodes. In this paper, we highlight an inherent problem in GNNs: the mechanism of propagating information between neighbors creates a *bottleneck* when every node aggregates messages from its neighbors. This bottleneck causes the *over-squashing* of exponentially-growing information into fixed-size vectors. As a result, the graph fails to propagate messages flowing from distant nodes and performs poorly when the prediction task depends on long-range information. We demonstrate that the bottleneck hinders popular GNNs from fitting the training data. We show that GNNs that absorb incoming edges equally, like GCN and GIN, are more susceptible to over-squashing than other GNN types. We further show that existing, extensively-tuned, GNN-based models suffer from over-squashing and that breaking the bottleneck improves state-of-the-art results without any hyperparameter tuning or additional weights.

1 Introduction

Graph neural networks (GNNs) (Scarselli et al., 2008; Micheli, 2009) have seen growing popularity over the last few years (Duvenaud et al., 2015; Hamilton et al., 2017; Xu et al., 2019). Many domains can be naturally represented as graphs. Therefore, GNNs provide a convenient and general framework to model a variety of real-world complex structural data such as social networks, knowledge graphs, computer programs, and chemical and biological systems.

A GNN layer can be viewed as a message-passing step (Gilmer et al., 2017), where each node updates its state by aggregating messages flowing from its neighbors. GNN variants (Li et al., 2016; Veličković et al., 2018; Kipf and Welling, 2017) mostly differ in how each node aggregates the representations of its neighbors and combines them with its own representation. In this paper, we show that this message-passing mechanism creates a numerical information *bottleneck* when computing neighbor aggregation. Problems that depend on long-range interaction between nodes must use as many GNN layers as the desired radius of a node’s receptive field. Unfortunately, the number of nodes in the receptive field grows *exponentially* with the number of layers. This causes *over-squashing*: information from the exponentially-growing receptive field is compressed into fixed-length vectors. Consequently, the graph fails to propagate messages flowing from distant nodes; the model overfits on other signals in the training data instead; and overall, the model performs poorly.

In fact, the GNN bottleneck is analogous to the bottleneck of sequential recurrent models. Traditional seq2seq models (Sutskever et al., 2014; Cho et al., 2014a,b) suffered from a bottleneck at every decoder state – the model had to encapsulate the entire input sequence into a fixed-size vector. In GNNs, the bottleneck is even more harmful, because the receptive field of a node grows exponentially

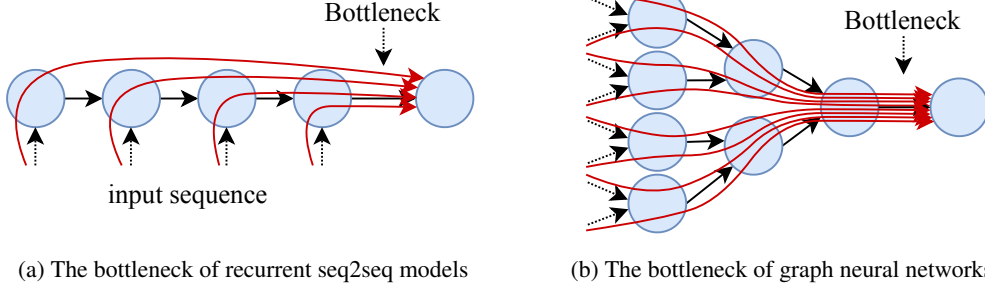


Figure 1: The bottleneck of recurrent seq2seq models (before attention) is more harmful in GNNs: information from a node’s exponentially-growing receptive field is compressed into a fixed-size vector. Black arrows are graph edges; red curved arrows illustrate information flow.

with the number of message propagation steps, rather than linearly as in recurrent models. This difference is illustrated in Figure 1.

This work does *not* aim to propose a new GNN variant. Rather, the main contribution of this work is highlighting the inherent bottleneck problem of GNNs and studying its over-squashing implications. We use a controlled synthetic problem to demonstrate the existence of a bottleneck and to provide combinatorial upper bounds for the graph size given the network’s hidden dimension (Section 5). We show, analytically and empirically, that GCN (Kipf and Welling, 2017) and GIN (Xu et al., 2019) suffer from over-squashing *more* than other types of GNNs, and even in small graphs. We further show that existing models of real-world datasets suffer from over-squashing: breaking the bottleneck relatively reduces the error rate by 42% in the QM9 dataset, by 12% in the ENZYMES dataset, and by 4.8% in the NCI1 dataset, without any hyperparameter tuning nor additional weights.

2 Preliminaries

A directed graph $\mathcal{G} = (\mathcal{V}, \mathcal{E})$ contains nodes \mathcal{V} and edges \mathcal{E} , where $(u, v) \in \mathcal{E}$ denotes an edge from a node u to a node v . For brevity, in the following definitions we treat all edges as having the same *type*; in general, every edge can have a type and features (Schlichtkrull et al., 2018).

Graph neural networks Graph neural networks operate by propagating neural messages between neighboring nodes. At every propagation step (a graph layer): the network computes each node’s sent message; every node aggregates its received messages; and each node updates its representation by combining the aggregated incoming messages with its own previous representation.

Formally, each node is associated with an initial representation $\mathbf{h}_v^{(0)} \in \mathcal{R}^{d_0}$. This representation is usually derived from the node’s label or its given features. Then, a GNN layer updates each node’s representation given its neighbors, yielding $\mathbf{h}_v^{(1)} \in \mathcal{R}^d$. In general, the k -th layer of a GNN is a parametric function f_k that is applied to each node by considering its neighbors:

$$\mathbf{h}_v^{(k)} = f_k \left(\mathbf{h}_v^{(k-1)}, \{ \mathbf{h}_u^{(k-1)} \mid u \in \mathcal{N}_v \}; \theta_k \right) \quad (1)$$

where \mathcal{N}_v is the set of nodes that have edges to v : $\mathcal{N}_v = \{u \in \mathcal{V} \mid (u, v) \in \mathcal{E}\}$. The total number of layers K is usually determined empirically as a hyperparameter.

The design of the function f is what mostly distinguishes one type of GNN from the other. For example, graph convolutional networks (GCN) (Kipf and Welling, 2017) define f as:

$$\mathbf{h}_v^{(k)} = \sigma \left(\frac{1}{c_{u,u}} W^{(k)} \mathbf{h}_v^{(k-1)} + \sum_{u \in \mathcal{N}_v} \frac{1}{c_{u,v}} W^{(k)} \mathbf{h}_u^{(k-1)} \right) \quad (2)$$

where σ is a nonlinearity such as *ReLU*, and $c_{u,v}$ is a normalization factor often set to $|\mathcal{N}_v|$ or $\sqrt{|\mathcal{N}_v| \cdot |\mathcal{N}_u|}$. As another example, graph isomorphism networks (GIN) (Xu et al., 2019) update a node’s representation using the following definition:

$$\mathbf{h}_v^{(k)} = MLP^{(k)} \left(\left(1 + \epsilon^{(k)} \right) \mathbf{h}_v^{(k-1)} + \sum_{u \in \mathcal{N}_v} \mathbf{h}_u^{(k-1)} \right) \quad (3)$$

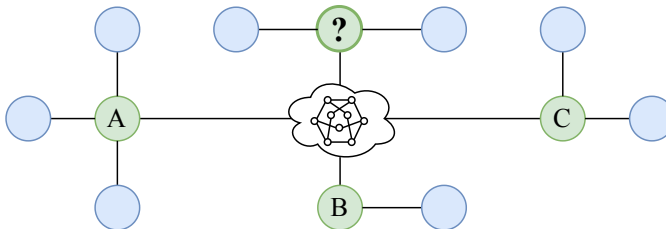



Figure 2: An example NEIGHBORSMATCH problem. Green nodes (A, B, C) have blue neighbors (●) and an alphabetical label. The goal is to predict the label C for the target node (?), because the target node has *two* blue neighbors, like the node marked with C in the same graph.

Usually, the last (K -th) layer’s output is used for prediction: in node-prediction tasks, $\mathbf{h}_v^{(K)}$ is used to predict a label for v ; in graph-prediction tasks, a permutation-invariant “readout” function aggregates the nodes of the final layer using summation, averaging, or a weighted sum (Li et al., 2016).

3 The GNN Bottleneck

When a prediction problem relies on long-range interaction between nodes, the GNN is required to have as many layers as the estimated length of these interactions. However, the number of nodes in the receptive field of a node grows exponentially with the number of layers. As a result, an exponentially-growing amount of information is squashed into a fixed-length vector (i.e., the result of the \sum in Equations (2) and (3)), and crucial messages fail to reach their distant destinations. Instead, the model may overfit on other signals in the training data and overall generalize poorly at test time.

For example, consider the NEIGHBORSMATCH problem of Figure 2. Green nodes (A, B, C) have a varying number of blue neighbors (●) and an alphabetical label. Every example in the dataset has a different mapping from numbers of neighbors to labels. The rest of the graph (marked as ) represents a general, unknown, graph structure. The goal is to predict a label for the target node, which is marked with a question mark (?), according to its number of blue neighbors. The correct answer is C in this case, because the target node has *two* blue neighbors, like the node marked with C in the same graph. Since the model has to propagate information from *all* green nodes before predicting the label, a bottleneck at the target node is inevitable. This bottleneck causes *over-squashing*, which can prevent the model from fitting the training data, even though the desired prediction is obvious in a global view. We demonstrate the bottleneck empirically in an instance of this problem in Section 4; in Section 5, we provide upper bounds for the learnable graph size.

Although this is a contrived problem, it resembles real-world problems that are often modeled as graphs. For example, a computer program in a language such as Python may declare multiple variables (i.e., the green nodes in Figure 2) along with their types and values (their numbers of blue neighbors in Figure 2); later in the program, predicting which variable should be used in a specific location (predict the alphabetical label in Figure 2) must use one of the available variables based on the required type and the required value at that point (Allamanis et al., 2018).

Short- vs. long-range problems Much of prior GNN work has focused on problems that were local in nature, where the underlying inductive bias was that a node’s most relevant context is its local neighborhood, and long-range interaction was not necessarily needed. With the growing popularity of GNNs, their adoption expanded to domains that required longer-range information propagation as well, without addressing the inherent bottleneck. In this paper, we focus on problems that *require* long-range information. That is, a correct prediction requires considering the local environment of a node *and* interactions beyond the close neighborhood. For example, a chemical property of a molecule can depend on the combination of atoms that reside in the molecule’s *opposite sides* (Ramakrishnan et al., 2014; Gilmer et al., 2017). Problems of this kind require long-range interaction, and thus, a large number of GNN layers. As the receptive field of each node grows exponentially with the number of layers – the more layers, the more harmful the effect of the bottleneck.

In problems that are local in nature – the bottleneck is less troublesome, because information does not need to flow across long paths, and the receptive field of a node can be exponentially smaller.

Domains such as citation networks (Sen et al., 2008), social networks (Leskovec and McAuley, 2012), movie collaboration (Yanardag and Vishwanathan, 2015), and product recommendations (Shchur et al., 2018) usually raise short-range problems and are thus *not* the focus of this paper.

4 Evaluation

Bottleneck in synthetic problems First, we wish to empirically show that the GNN bottleneck exists, and even in small graphs. We generated a synthetic benchmark that is theoretically solvable; however, in practice, all GNNs fail to reach 100% training accuracy because of the bottleneck (Section 4.1).


Bottleneck in existing models Second, we examine whether the bottleneck exists in prior models, which addressed real-world problems (Sections 4.2 and 4.3). To that end, we wish to measure over-squashing in existing models. But, how can we measure over-squashing? We measure whether breaking the bottleneck improves the results.

Adding a fully-adjacent layer (FA) We took off-the-shelf, extensively tuned, models, and modified adjacency in the last layer by modifying the authors’ original code: given a GNN with K layers, we modified the K -th layer to be a *fully-adjacent layer*. A *fully-adjacent layer* is a GNN layer in which every pair of nodes is connected by an edge. In terms of Equations (1) to (3), converting an existing layer to be fully-adjacent means that $\mathcal{N}_v := \mathcal{V}$ for every node $v \in \mathcal{V}$, only in that layer. This does not change the type of layer nor add weights, but only changes the notion of adjacency of a data sample in a single layer. Thus, the $K - 1$ graph layers exploit the graph structure using their original sparse topology, and only the K -th layer is an FA layer that allows the topology-aware nodes to interact directly and consider nodes beyond their original neighbors. Hopefully, this would ease information flow, prevent over-squashing, and reduce the effect of the previously-existed bottleneck.

We re-trained the models without performing *any* additional tuning, to rule out hyperparameter tuning as the source of improvement. This approach allows approximating the effect of the bottleneck on the original model without changing the graph topology or adding weights. We emphasize that our goal is *not* to pinpoint the best GNN type; but rather, to measure the negative effect of the bottleneck in the original models. Statistics of all datasets can be found in the supplementary material.

4.1 Synthetic Benchmark: NEIGHBORMATCH

The NEIGHBORMATCH problem (Figure 2) is a simple contrived problem that we designed to demonstrate that over-squashing affects even small graphs. We focus on the *training* accuracy of a model and show that the bottleneck prevents models from fitting the training set.

TREE-NEIGHBORMATCH We created an instance of the general NEIGHBORMATCH problem that we described in Section 3 and portrayed in Figure 2. As observed before (Micheli, 2009; Chen et al., 2018), the receptive field of a node in a graph grows exponentially with the number of layers. Thus, from the perspective of a single node v , the rest of the graph may look like a tree, rooted at v (Garg et al., 2020). To simulate this exponentially-growing receptive field, we instantiated the subgraph in the middle of the graph (marked as  in Figure 2) as a binary tree of depth $depth$ where the green nodes are its leaves, and the target node is the tree’s root. All edges are directed toward the root, such that information is propagated from all nodes toward the target node. The goal, as in Section 3, is to predict a label for the target node, where the correct answer is the label of the green node that has the same number of blue neighbors as the target node. An illustration is shown in Figure 5 in the supplementary material. In this section we observe the bottleneck empirically; in Section 5 we provide a combinatorial upper bound for the learnable graph size in this problem.

Data We created a separate dataset for every $depth$ and sampled up to 32,000 examples per dataset. The label of each leaf (“A”, “B”, “C” in Figure 2) is represented as a one-hot vector. To tease the effect of the bottleneck from the ability of a GNN to count neighbors, we concatenated each leaf node’s initial representation with a 1-hot vector representing the number of blue neighbors, instead of creating the blue nodes. The target node is initialized with an all-zeros vector as its (missing) label, concatenated with a 1-hot vector representing its number of blue neighbors. Intermediate nodes are initialized with a vector of zeros.

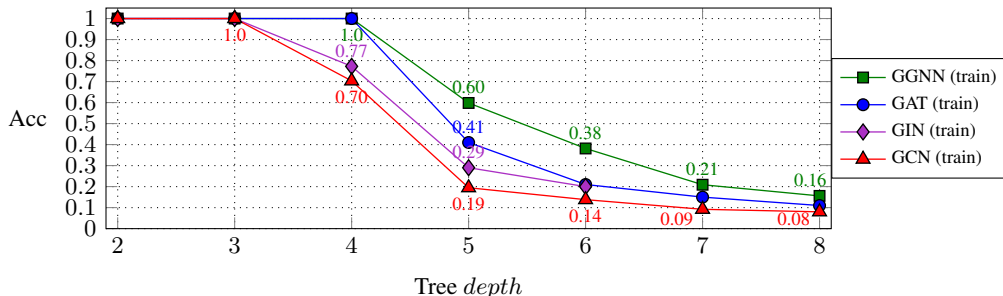


Figure 3: Accuracy across tree *depth* in the NEIGHBORSMATCH problem (Section 4.1). The bottleneck starts to affect the vanilla GCN even at *depth* = 4.

Model We implemented a network with an initial linear layer, followed by *depth*+1 graph layers to allow an additional nonlinear layer after the information from the leaves reaches the target node. We experimented with GCN (Kipf and Welling, 2017), GGNN (Li et al., 2016), GIN (Xu et al., 2019) and GAT (Veličković et al., 2018) as the graph layers. The final target node representation goes through a linear layer and a softmax to predict its label. We make our PyTorch Geometric (Fey and Lenssen, 2019) implementation publicly available

We used model dimensions of $d=32$. Larger values lead to the exact same trend. We further discuss the theoretical and empirical aspects of the dimension in Section 5. We added residual connections, summing every node with its own representation in the previous layer to increase expressivity, and layer normalization which eased convergence. We used the Adam optimizer with a learning rate of 10^{-3} , decayed by 0.5 after every 1000 epochs without an increase in training accuracy, and stopped training after 2000 epochs of no training accuracy improvement.

Results Figure 3 shows the following surprising results: GNNs fail to fit the dataset starting from *depth*=4. For example, the training accuracy of GCN at *depth*=4 is 70%. At *depth*=5, all GNNs fail to perfectly fit the data. Starting from *depth*=4, the models suffered from *over-squashing* that resulted in *underfitting*: the bottleneck prevented the models from distinguishing between different training examples, even after they were observed tens of thousands of times. These results clearly show the existence of the bottleneck and its negative effect, even in small graphs.

Discussion GCN and GIN managed to perfectly fit *depth*=3 at most, while GGNN and GAT also reached 100% accuracy at *depth*=4. This difference can be explained by their neighbor aggregation computation: consider the target node that receives messages in the *depth*'th step. GCN and GIN aggregate all neighbors *before* combining them with the target node's representation, and thus they must compress the information flowing from *all* leaves into a single vector, and *only afterward* interact with the target node's own representation (Equations (2) and (3)). In contrast, a GAT layer uses the target's own representation to weight incoming messages; the target node can thus ignore the irrelevant incoming edge and absorb only the relevant incoming edge, which contains information flowing from *half* of the leaves. Following Levy et al. (2018), we hypothesize that the GRU cell in GGNNs filters incoming edges as GAT, but perform this filtering as element-wise attention. Since the number of leaves grows exponentially with *depth*, it is expected that GNNs that need to compress *only half* of the information (GGNN and GAT) will succeed at a *depth* that is larger by 1.

If all GNNs have reached low training accuracy in small depths, how do GNN-based models usually do reach high training accuracy in public datasets? We hypothesize that they overfit on other signals in the training set, rather than learning the information that was squashed in the bottleneck.

4.2 Quantum Chemistry: QM9

Data The QM9 dataset (Ramakrishnan et al., 2014; Gilmer et al., 2017; Wu et al., 2018) contains ~130,000 graphs with ~18 nodes. Each graph is a molecule where nodes are atoms, and undirected, typed edges are different types of bonds between the atoms. The goal is to regress each graph to 13 real-valued quantum chemical properties such as *dipole moment* and *isotropic polarizability*.

Property	GNN-MLP0		R-GAT		GNN-FiLM	
	base [†]	+FA	base [†]	+FA	base [†]	+FA
mu	2.36±0.04	2.19 ±0.04	2.68 ±0.06	2.73±0.07	2.38±0.13	2.26 ±0.06
alpha	4.27±0.36	1.92 ±0.06	4.65±0.44	2.32 ±0.16	3.75±0.11	1.93 ±0.08
HOMO	1.25±0.04	1.19 ±0.04	1.48±0.03	1.43 ±0.02	1.22±0.07	1.11 ±0.01
LUMO	1.35±0.04	1.20 ±0.05	1.53±0.07	1.41 ±0.03	1.30±0.05	1.21 ±0.05
gap	2.04±0.05	1.82 ±0.05	2.31±0.06	2.08 ±0.05	1.96±0.06	1.79 ±0.07
R2	14.86±1.62	12.40 ±0.84	52.39 ±42.5	15.76 ±1.17	15.59±1.38	11.89 ±0.73
ZPVE	12.00±1.66	4.68 ±0.29	14.87±2.88	5.98 ±0.43	11.00±0.74	4.68 ±0.49
U0	5.55±0.38	1.71 ±0.13	7.61±0.46	2.19 ±0.25	5.43±0.96	1.60 ±0.12
U	6.20±0.88	1.72 ±0.12	6.86±0.53	2.11 ±0.10	5.95±0.46	1.75 ±0.08
H	5.96±0.45	1.70 ±0.08	7.64±0.92	2.27 ±0.29	5.59±0.57	1.93 ±0.42
G	5.09±0.57	1.53 ±0.15	6.54±0.36	2.07 ±0.07	5.17±1.13	1.77 ±0.05
Cv	3.38±0.20	1.69 ±0.08	4.11±0.27	2.03 ±0.14	3.46±0.21	1.64 ±0.10
Omega	0.84±0.02	0.63 ±0.04	1.48±0.87	0.73 ±0.04	0.98±0.06	0.69 ±0.05
Relative:		-40.33%		-44.58%		-39.53%

Table 1: Average error rates (for each property: 5 runs \pm stdev) on the QM9 dataset. The best result for every property in every GNN type is highlighted in bold. Results marked with [†] were previously reported by Brockschmidt (2020) and reproduced by us.

Models We used the implementation of Brockschmidt (2020) who performed an extensive hyperparameter tuning for multiple GNNs, by searching over 500 configurations; we took the same training/validation/test splits and their best-found configurations. For most GNNs, Brockschmidt found that the best results are achieved using *eight* propagation steps. This led us to hypothesize that this problem depends on long-range information and relies on both graph structure *and* distant nodes.

We experimented with GNN-MLP0, R-GAT, GNN-FiLM (Brockschmidt, 2020), GGNN, R-GCN (Schlichtkrull et al., 2018) and R-GIN. For every target property – Brockschmidt found that either GNN-MLP0 or GNN-FiLM achieved the best (lowest) error rate. We modified the last layer to be an FA layer by extending their implementation. We re-trained each modified model for each target property using the same code, configuration, and training scheme as Brockschmidt (2020), training each model five times (using different random seeds) for each target property task. We compare the “base” models, reported by Brockschmidt, with our modified and re-trained “+FA” models.

Results Results for the top GNNs are shown in Table 1; results for the other GNNs are shown in Table 4 in the supplementary material due to space limitation. The main results are that breaking the bottleneck by modifying a single layer to be an FA layer significantly reduces the error rate, by 42% on average, across all GNNs. In GNN-MLP0 and GNN-FiLM – the improvement is consistent across all 13 target properties. In R-GAT - adding the FA layer improves in 12 out of the 13 target properties. These experiments clearly show evidence for a bottleneck in the original GNN models.

If all GNNs benefit from direct interaction between all nodes, maybe the graph structure is not even needed? We trained another set of models (not shown due to space limitation) where *all layers* are FA layers, ignoring the original graph structure; these models produced significantly worse results.

Over-squashing or under-reaching? Barceló et al. (2020) discuss the inability of a GNN node to be aware of nodes that are farther away than the number of layers K . We denote this limitation as *under-reaching*: for every fixed number of layers K , local information cannot travel farther than distance K along edges in the graph. So, was the significant improvement of the FA layer in Table 1 achieved thanks to the reduction in over-squashing, or did the FA layer only extend the nodes’ reachability and prevent under-reaching? To answer this question, we measured the graphs’ *diameter* in the QM9 dataset – the maximum shortest path between two nodes in a graph. We found that the average diameter is 6.35 ± 0.91 , the maximum diameter is 10, and the 90th percentile is 8, while most models were trained with 8 layers. That is, at least 90% of the examples in the dataset certainly did *not* suffer from under-reaching, because the number of layers was greater or equal than their diameter. We trained another set of models (not shown due to space limitation) with 10 layers, which did not show significant improvement over the base models. We conclude that the source of improvement was clearly *not* the increased reachability, but instead, the reduction in over-squashing.

		NCI1	ENZYMES
No Struct [†]		69.8 ± 2.2	65.2 ± 6.4
DiffPool	base [†]	76.9 ± 1.9	59.5 ± 5.6
	+FA	77.6 ± 1.3	65.7 ± 4.8
GraphSAGE	base [†]	76.0 ± 1.8	58.2 ± 6.0
	+FA	77.7 ± 1.8	60.8 ± 4.5
DGCNN	base [†]	76.4 ± 1.7	38.9 ± 5.7
	+FA	76.8 ± 1.5	42.8 ± 5.3
GIN	base [†]	80.0 ± 1.4	59.6 ± 4.5
	+FA	81.5 ± 1.2	67.7 ± 5.3

Table 2: Average accuracy (30 runs ± stdev) on the biological datasets. Rows marked with [†] were previously reported by Errica et al. (2020).

4.3 Biological Benchmarks

Data We experimented with two popular biological datasets. NCI1 (Wale et al., 2008) contains ~30 nodes and its task is to predict whether a biochemical compound contains anti-lung-cancer activity. ENZYMES (Borgwardt et al., 2005) contains ~36 nodes and its task is to classify an enzyme to one out of six classes. We used the same 10-folds and training/validation/test split as Errica et al. (2020).

Models We used the implementation of Errica et al. (2020) who performed a fair and thorough comparison between GNNs by splitting each dataset to 10-folds; then, for each GNN type they select a configuration among a grid of 72 configurations according to the validation set; finally, the best configuration for each fold is trained three additional times, early stopped using the validation set, and evaluated on the test set. The final reported result is the average of all 30 test runs (10-folds×3).

In ENZYMES, Errica et al. found that a baseline that does not use the graph topology *at all* (“No Struct”) performs better than all GNNs. In NCI1, GIN performed best. We converted the last layer into an FA layer by modifying the implementation of Errica et al., and repeated the same training procedure. We compare the “base” models from Errica et al. with our re-trained “+FA” models.

Results Results are shown in Table 2. The main results are as follows: (a) in NCI1, GIN+FA improves by 1.5% over GIN-base, which was previously the best performing model; (b) in ENZYMES, where Errica et al. (2020) found that none of the GNNs exploit the topology of the graph, we find that GIN+FA *does* exploit the structure and improves by 8.1% over GIN-base and by 2.5% over *No Struct*. On average, models with FA layers relatively reduce the error rate by 12% in ENZYMES and by 4.8% in NCI1. These experiments clearly show evidence for a bottleneck in the original GNN models.

5 Combinatorial Analysis

In this section, we analyze the bottleneck combinatorially in the TREE-NEIGHBORSMATCH problem. We provide a combinatorial upper bound for the maximal depth that a GNN can perfectly fit (learn to 100% training accuracy) given its hidden vector size d . We denote the arity of such a tree by m ; the counting base as b ; the number of bits in a floating-point variable as f ; and the hidden dimension of the GNN, i.e., the size of a node vector $\mathbf{h}_v^{(k)}$, as d .

A full tree of arity m has m^{depth} leaves. As described in Section 4.1, given an arrangement of blue neighbors, all possible permutations of the labels $\{A, B, C, \dots\}$ are valid. Thus, the number of leaf label assignments is $(m^{\text{depth}})!$. Right before interacting with the target node and predicting the label, a single vector of size d must encapsulate the information flowing from all leaves (Equations (2) and (3)).¹ Such a vector contains d floating-point elements, each of them is stored as f bits. Overall,

¹The analysis holds for GCN and GIN. Architectures that use the representation of the recipient node to aggregate messages, like GAT, need to compress the information from only *half* of the leaves in a single vector. This increases the final upper bounds of depth by up to 1 and demonstrated empirically in Section 4.1.

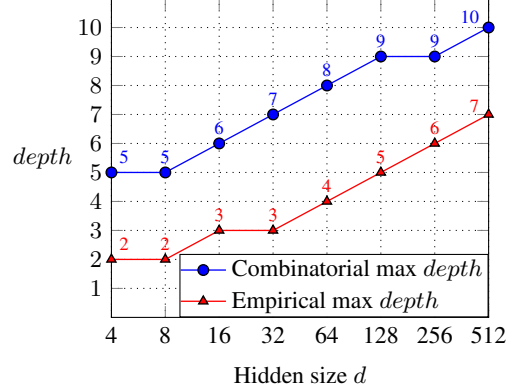


Figure 4: The combinatorial and empirical upper bounds of depth given d – the model dimension.

the number of possible cases that this vector can distinguish between is $b^{f \cdot d}$. The number of possible cases that the vector can distinguish between must be greater than the number of different examples this vector may encounter in the training data. Thus, $depth$ and d must satisfy Equation (4); considering binary trees ($m=2$), and floating-point values of $f=32$ binary ($b=2$) bits, we get Equation (5):

$$(m^{depth})! < b^{f \cdot d} \quad (4) \quad (2^{depth})! < 2^{32 \cdot d} \quad (5)$$

Since factorial grows faster than an exponent with a constant base, we can see that a small increase of $depth$ requires a much larger increase in d . Specifically, it means that for $d=32$ as in the experiments in Section 4.1, the combinatorial upper bound of the model is as low as $depth=7$. That is, a model with $d=32$ *cannot* obtain 100% accuracy for $depth \geq 8$. In practice, the problem is worse; i.e., the empirical upper bound is lower, because even if a solution to storing some information in a vector of a certain size exists, it is not guaranteed that a gradient descent-based algorithm will find it.

Figure 4 shows the combinatorial upper bounds for $depth$ given $d \in \{4, 8, 16, 32, 64, 128, 256, 512\}$. We repeated the experiments from Section 4.1 and report the max *empirical depth* for each value of d . As shown in Figure 4, even with $d=512$, the combinatorial upper bound is as low as $depth=10$.

6 Related Work

Under-reaching Although GNNs can be as powerful as the Weisfeiler-Lehman graph isomorphism test (Morris et al., 2019; Xu et al., 2019; Maron et al., 2019), their expressiveness captures only a small fragment of first-order logic (Barceló et al., 2020); the main limitation arises from the inability of a node to be aware of nodes that are farther away than the number of layers K , while the existence of such nodes *can* be easily described using logic. We denote this limitation as *under-reaching*. The *over-squashing* limitation described in this paper is *tighter*: even when information is reachable within K edges, this information might fail to flow in the bottleneck (as we demonstrate in Section 4.2).

Over-smoothing The *over-smoothing* phenomenon is related, but not identical, to over-squashing: node representations become indistinguishable and prediction performance severely degrades when the number of layers increases (Li et al., 2018; Klicpera et al., 2019; Wu et al., 2020; Oono and Suzuki, 2020). Several approaches were proposed to mitigate over-smoothing, such as normalization (Zhao and Akoglu, 2020), edge-based dropout (Rong et al., 2020), and noise-reduction regularization (Chen et al., 2020). This might explain the empirical optimality of few layers (e.g., only two layers in Kipf and Welling (2017)); however, some problems depend on longer-range information propagation and thus require more layers, such as those examined in Section 4. The bottleneck that we describe in this paper is an orthogonal problem to over-smoothing in tasks that rely on long-range information.

Avoiding over-squashing Gilmer et al. (2017) add “virtual edges” to shorten long distances, and Scarselli et al. (2008) add “supersource nodes”; however, these were mostly ad hoc solutions. Nikolentzos et al. (2019) update a node’s representation by recursively aggregating information from “k-hop” neighbors away at every layer in a computationally expensive approach, which forces k to be 2 or 3 at the most. Allamanis et al. (2018) designed program analyses that serve as 16 “shortcut” edge types; however, these analyses are specific to their problem and require a human domain expert. Although some previous work avoided over-squashing by various profitable means, none of these works explicitly identified the bottleneck and its negative cross-domain implications.

7 Conclusion

We highlight an inherent bottleneck problem that limits graph neural networks and causes over-squashing. Problems that depend on long-range interaction require as many GNN layers as the desired radius of each node’s receptive field. This causes an exponentially-growing amount of information to be squashed into a fixed-length vector. As a result, the graph fails to propagate long-range information and performs poorly when the prediction task depends on long-range interaction.

We demonstrate the existence of the bottleneck in a synthetic problem and show that GCN and GIN are more susceptible to over-squashing than other GNNs. We analyze this problem combinatorially and provide upper bounds for the tree depth. We further show that models of popular chemical and biological benchmarks suffer from the bottleneck, by showing that they can be dramatically improved by modifying a single layer to be fully-adjacent, and re-training without any hyperparameter tuning.

Acknowledgments

We would like to thank Federico Errica for his help in using his framework; Petar Veličković for helpful discussions about GAT; and Jorge Perez for helpful discussions about the expressiveness of GNNs. We are also grateful to (alphabetically): Chen Zarfati, Elad Nachmias, Gail Weiss, Lotem Fridman, Roy Sadaka, Shaked Brody, and Yoav Goldberg for their useful comments on an earlier version of this paper.

Supplementary Material

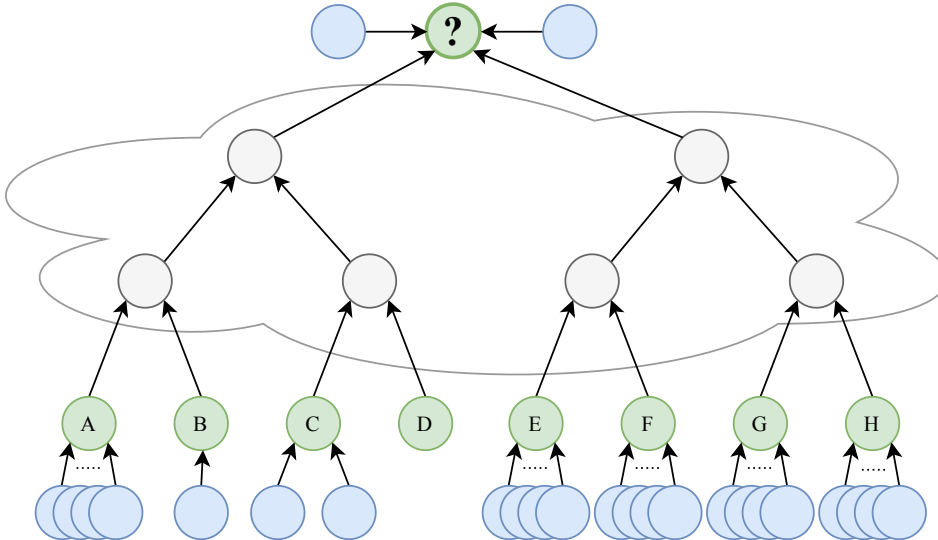


Figure 5: An example of a TREE-NEIGHBORSMATCH, that is an instance of the general NEIGHBORSMATCH problem that we examine in Section 4 of the paper. The target node (?) is the root of a tree of $depth=3$ (from the target node to the green nodes). The green nodes (A, B, C, ...) have blue neighbors (○) and an alphabetical label. The node B has a single blue neighbor; the node C has *two* blue neighbors; and the node D has no blue neighbors; each other green node has another unique number of blue neighbors. The goal is to predict a label for the target node (?) according to its number of blue neighbors. The correct answer is C in this example, because the target node has two blue neighbors, like the green node that is marked with C in the same graph. To make a correct prediction, the network must propagate information from *all* leaves toward the target node, and make the decision given a single fixed-sized vector that compresses all this information.

8 QM9 - Additional Results

Because of space limitations, in Section 4.2 we presented results on the QM9 dataset only for GNN-MLP0, R-GAT and GNN-FiLM. In this section, we show that additional GNN architectures benefit from breaking the bottleneck using a fully-adjacent layer: GGNN (Li et al., 2016), R-GCN (Schlichtkrull et al., 2018) and R-GIN (Xu et al., 2019).

Table 3 is identical to Table 1 and contains results for GNN-MLP0, R-GAT and GNN-FiLM. Table 4 contains additional results for GGNN, R-GCN and R-GIN. As shown in Table 4, adding an FA layer significantly improves results across all GNN architectures, for all properties except for “mu” in R-GAT, where adding an FA layer results in a slightly higher error rate.

9 Data Statistics

9.1 Synthetic Dataset: TREE-NEIGHBORSMATCH

Statistics of the synthetic TREE-NEIGHBORSMATCH dataset are shown in Table 5.

Property	GNN-MLP0		R-GAT		GNN-FiLM	
	base [†]	+FA	base [†]	+FA	base [†]	+FA
mu	2.36±0.04	2.19 ±0.04	2.68 ±0.06	2.73±0.07	2.38±0.13	2.26 ±0.06
alpha	4.27±0.36	1.92 ±0.06	4.65±0.44	2.32 ±0.16	3.75±0.11	1.93 ±0.08
HOMO	1.25±0.04	1.19 ±0.04	1.48±0.03	1.43 ±0.02	1.22±0.07	1.11 ±0.01
LUMO	1.35±0.04	1.20 ±0.05	1.53±0.07	1.41 ±0.03	1.30±0.05	1.21 ±0.05
gap	2.04±0.05	1.82 ±0.05	2.31±0.06	2.08 ±0.05	1.96±0.06	1.79 ±0.07
R2	14.86±1.62	12.40 ±0.84	52.39 ±42.5	15.76 ±1.17	15.59±1.38	11.89 ±0.73
ZPVE	12.00±1.66	4.68 ±0.29	14.87±2.88	5.98 ±0.43	11.00±0.74	4.68 ±0.49
U0	5.55±0.38	1.71 ±0.13	7.61±0.46	2.19 ±0.25	5.43±0.96	1.60 ±0.12
U	6.20±0.88	1.72 ±0.12	6.86±0.53	2.11 ±0.10	5.95±0.46	1.75 ±0.08
H	5.96±0.45	1.70 ±0.08	7.64±0.92	2.27 ±0.29	5.59±0.57	1.93 ±0.42
G	5.09±0.57	1.53 ±0.15	6.54±0.36	2.07 ±0.07	5.17±1.13	1.77 ±0.05
Cv	3.38±0.20	1.69 ±0.08	4.11±0.27	2.03 ±0.14	3.46±0.21	1.64 ±0.10
Omega	0.84±0.02	0.63 ±0.04	1.48±0.87	0.73 ±0.04	0.98±0.06	0.69 ±0.05
relative	-40.33%		-44.58%		-39.53%	

Table 3: Average error rates and standard deviations on the QM9 targets. Best result for every property in every GNN type is highlighted in bold. Results marked with [†] were previously reported by Brockschmidt (2020).

Property	GGNN		R-GCN		R-GIN	
	base [†]	+LLC	base [†]	+LLC	base [†]	+LLC
mu	3.85±0.16	3.53 ±0.13	3.21±0.06	2.92 ±0.07	2.64±0.11	2.54 ±0.09
alpha	5.22±0.86	2.72 ±0.12	4.22±0.45	2.14 ±0.08	4.67±0.52	2.28 ±0.04
HOMO	1.67±0.07	1.45 ±0.04	1.45±0.01	1.37 ±0.02	1.42±0.01	1.26 ±0.02
LUMO	1.74±0.06	1.63 ±0.06	1.62±0.04	1.41 ±0.01	1.50±0.09	1.34 ±0.04
gap	2.60±0.06	2.30 ±0.05	2.42±0.14	2.03 ±0.03	2.27±0.09	1.96 ±0.04
R2	35.94±35.68	14.33 ±0.47	16.38±0.49	13.55 ±0.50	15.63±1.40	12.61 ±0.37
ZPVE	17.84±3.61	5.24 ±0.30	17.40±3.56	5.81 ±0.61	12.93±1.81	5.03 ±0.36
U0	8.65±2.46	3.35 ±1.68	7.82±0.80	1.75 ±0.18	5.88±1.01	2.21 ±0.12
U	9.24±2.26	2.49 ±0.34	8.24±1.25	1.88 ±0.22	18.71±23.36	2.32 ±0.18
H	9.35±0.96	2.31 ±0.15	9.05±1.21	1.85 ±0.18	5.62±0.81	2.26 ±0.19
G	7.14±1.15	2.17 ±0.29	7.00±1.51	1.76 ±0.15	5.38±0.75	2.04 ±0.24
Cv	8.86±9.07	2.25 ±0.20	3.93±0.48	1.90 ±0.07	3.53±0.37	1.86 ±0.03
Omega	1.57±0.53	0.87 ±0.09	1.02±0.05	0.75 ±0.04	1.05±0.11	0.80 ±0.04
relative	-47.42%		-43.40%		-39.54%	

Table 4: Average error rates and standard deviations on the QM9 targets. Best result for every property in every GNN type is highlighted in bold. Results marked with [†] were previously reported by Brockschmidt (2020).

Table 5: The number of examples, in our experiments and combinatorially, for every value of *depth*.

<i>depth</i>	# Training examples sampled	Total combinatorial: $(2^{depth})! \cdot 2^{depth}$
2	96	96
3	8000	$> 3 \cdot 10^5$
4	16,000	$> 3 \cdot 10^{14}$
5	32,000	$> 10^{36}$
6	32,000	$> 10^{90}$
7	32,000	$> 10^{217}$
8	32,000	$> 10^{509}$

9.2 Quantum Chemistry: QM9

Statistics of the quantum chemistry QM9 dataset, as used in Brockschmidt (2020) are shown in Table 6.

Table 6: Statistics of the QM9 chemical dataset (Ramakrishnan et al., 2014) as used by Brockschmidt (2020).

	Training	Validation	Test
# examples	110,462	10,000	10,000
# nodes - average	18.03	18.06	18.09
# nodes - standard deviation	2.9	2.9	2.9
# edges - average	18.65	18.67	18.72
# edges - standard deviation	3.1	3.1	3.1

9.3 Biological Benchmarks

Statistics of the biological datasets, as used in Errica et al. (2020), are shown in Table 7.

Table 7: Statistics of the biological datasets, as used by Errica et al. (2020).

	NCI1 (Wale et al., 2008)	ENZYMES (Borgwardt et al., 2005)
# examples	4110	600
# classes	2	6
# nodes - average	29.87	32.63
# nodes - standard deviation	13.6	15.3
# edges - average	32.30	64.14
# edges - standard deviation	14.9	25.5
# node labels	37	3

References

- Miltiadis Allamanis, Marc Brockschmidt, and Mahmoud Khademi. Learning to represent programs with graphs. In *International Conference on Learning Representations*, 2018. URL <https://openreview.net/forum?id=BJOFETxR->.
- Pablo Barceló, Egor V. Kostylev, Mikael Monet, Jorge Pérez, Juan Reutter, and Juan Pablo Silva. The logical expressiveness of graph neural networks. In *International Conference on Learning Representations*, 2020. URL <https://openreview.net/forum?id=r11Z7AEKvB>.
- Karsten M Borgwardt, Cheng Soon Ong, Stefan Schöner, SVN Vishwanathan, Alex J Smola, and Hans-Peter Kriegel. Protein function prediction via graph kernels. *Bioinformatics*, 21(suppl_1):i47–i56, 2005.
- Marc Brockschmidt. Gnn-film: Graph neural networks with feature-wise linear modulation. *Proceedings of the 36th International Conference on Machine Learning, ICML, 2020*.
- Deli Chen, Yankai Lin, Wei Li, Peng Li, Jie Zhou, and Xu Sun. Measuring and relieving the over-smoothing problem for graph neural networks from the topological view. In *Proceedings of the Thirty-Fourth Conference on Association for the Advancement of Artificial Intelligence (AAAI)*, 2020.
- Jianfei Chen, Jun Zhu, and Le Song. Stochastic training of graph convolutional networks with variance reduction. In *International Conference on Machine Learning*, pages 942–950, 2018.
- Kyunghyun Cho, Bart van Merriënboer, Dzmitry Bahdanau, and Yoshua Bengio. On the properties of neural machine translation: Encoder–decoder approaches. In *Proceedings of SSST-8, Eighth Workshop on Syntax, Semantics and Structure in Statistical Translation*, pages 103–111, 2014a.
- Kyunghyun Cho, Bart Van Merriënboer, Caglar Gulcehre, Dzmitry Bahdanau, Fethi Bougares, Holger Schwenk, and Yoshua Bengio. Learning phrase representations using rnn encoder-decoder for statistical machine translation. *arXiv preprint arXiv:1406.1078*, 2014b.

- David K Duvenaud, Dougal Maclaurin, Jorge Iparraguirre, Rafael Bombarell, Timothy Hirzel, Alán Aspuru-Guzik, and Ryan P Adams. Convolutional networks on graphs for learning molecular fingerprints. In *Advances in neural information processing systems*, pages 2224–2232, 2015.
- Federico Errica, Marco Podda, Davide Bacciu, and Alessio Micheli. A fair comparison of graph neural networks for graph classification. In *International Conference on Learning Representations*, 2020. URL <https://openreview.net/forum?id=HygDF6NFPB>.
- Matthias Fey and Jan E. Lenssen. Fast graph representation learning with PyTorch Geometric. In *ICLR Workshop on Representation Learning on Graphs and Manifolds*, 2019.
- Vikas K Garg, Stefanie Jegelka, and Tommi Jaakkola. Generalization and representational limits of graph neural networks. *arXiv preprint arXiv:2002.06157*, 2020.
- Justin Gilmer, Samuel S Schoenholz, Patrick F Riley, Oriol Vinyals, and George E Dahl. Neural message passing for quantum chemistry. In *Proceedings of the 34th International Conference on Machine Learning-Volume 70*, pages 1263–1272. JMLR. org, 2017.
- Will Hamilton, Zhitao Ying, and Jure Leskovec. Inductive representation learning on large graphs. In *Advances in neural information processing systems*, pages 1024–1034, 2017.
- Thomas N Kipf and Max Welling. Semi-supervised classification with graph convolutional networks. In *ICLR*, 2017.
- Johannes Klicpera, Aleksandar Bojchevski, and Stephan Günnemann. Combining neural networks with personalized pagerank for classification on graphs. In *International Conference on Learning Representations*, 2019. URL <https://openreview.net/forum?id=H1gL-2A9Ym>.
- Jure Leskovec and Julian J McAuley. Learning to discover social circles in ego networks. In *Advances in neural information processing systems*, pages 539–547, 2012.
- Omer Levy, Kenton Lee, Nicholas FitzGerald, and Luke Zettlemoyer. Long short-term memory as a dynamically computed element-wise weighted sum. In *Proceedings of the 56th Annual Meeting of the Association for Computational Linguistics (Volume 2: Short Papers)*, pages 732–739, 2018.
- Qimai Li, Zhichao Han, and Xiao-Ming Wu. Deeper insights into graph convolutional networks for semi-supervised learning. In *Thirty-Second AAAI Conference on Artificial Intelligence*, 2018.
- Yujia Li, Daniel Tarlow, Marc Brockschmidt, and Richard Zemel. Gated graph sequence neural networks. In *International Conference on Learning Representations*, 2016.
- Haggai Maron, Heli Ben-Hamu, Hadar Serviansky, and Yaron Lipman. Provably powerful graph networks. In *Advances in Neural Information Processing Systems*, pages 2153–2164, 2019.
- Alessio Micheli. Neural network for graphs: A contextual constructive approach. *IEEE Transactions on Neural Networks*, 20(3):498–511, 2009.
- Christopher Morris, Martin Ritzert, Matthias Fey, William L Hamilton, Jan Eric Lenssen, Gaurav Rattan, and Martin Grohe. Weisfeiler and leman go neural: Higher-order graph neural networks. In *Proceedings of the AAAI Conference on Artificial Intelligence*, volume 33, pages 4602–4609, 2019.
- Giannis Nikolentzos, George Dasoulas, and Michalis Vazirgiannis. k-hop graph neural networks. *ArXiv*, abs/1907.06051, 2019.
- Kenta Oono and Taiji Suzuki. Graph neural networks exponentially lose expressive power for node classification. In *International Conference on Learning Representations*, 2020. URL <https://openreview.net/forum?id=S1ld02EFPr>.
- Raghunathan Ramakrishnan, Pavlo O Dral, Matthias Rupp, and O Anatole Von Lilienfeld. Quantum chemistry structures and properties of 134 kilo molecules. *Scientific data*, 1:140022, 2014.
- Yu Rong, Wenbing Huang, Tingyang Xu, and Junzhou Huang. Dropedge: Towards deep graph convolutional networks on node classification. In *International Conference on Learning Representations*, 2020. URL <https://openreview.net/forum?id=Hkx1qkrKPr>.
- Franco Scarselli, Marco Gori, Ah Chung Tsoi, Markus Hagenbuchner, and Gabriele Monfardini. The graph neural network model. *IEEE Transactions on Neural Networks*, 20(1):61–80, 2008.

- Michael Schlichtkrull, Thomas N Kipf, Peter Bloem, Rianne Van Den Berg, Ivan Titov, and Max Welling. Modeling relational data with graph convolutional networks. In *European Semantic Web Conference*, pages 593–607. Springer, 2018.
- Prithviraj Sen, Galileo Namata, Mustafa Bilgic, Lise Getoor, Brian Galligher, and Tina Eliassi-Rad. Collective classification in network data. *AI magazine*, 29(3):93–93, 2008.
- Oleksandr Shchur, Maximilian Mumme, Aleksandar Bojchevski, and Stephan Günnemann. Pitfalls of graph neural network evaluation. *Relational Representation Learning Workshop, NeurIPS 2018*, 2018.
- Ilya Sutskever, Oriol Vinyals, and Quoc V Le. Sequence to sequence learning with neural networks. In *Advances in Neural Information Processing Systems*, pages 3104–3112, 2014.
- Petar Veličković, Guillem Cucurull, Arantxa Casanova, Adriana Romero, Pietro Liò, and Yoshua Bengio. Graph attention networks. In *International Conference on Learning Representations*, 2018. URL <https://openreview.net/forum?id=rJXmpikCZ>.
- Nikil Wale, Ian A Watson, and George Karypis. Comparison of descriptor spaces for chemical compound retrieval and classification. *Knowledge and Information Systems*, 14(3):347–375, 2008.
- Zhenqin Wu, Bharath Ramsundar, Evan N Feinberg, Joseph Gomes, Caleb Geniesse, Aneesh S Pappu, Karl Leswing, and Vijay Pande. Moleculenet: a benchmark for molecular machine learning. *Chemical science*, 9(2):513–530, 2018.
- Zonghan Wu, Shirui Pan, Fengwen Chen, Guodong Long, Chengqi Zhang, and S Yu Philip. A comprehensive survey on graph neural networks. *IEEE Transactions on Neural Networks and Learning Systems*, 2020.
- Keyulu Xu, Weihua Hu, Jure Leskovec, and Stefanie Jegelka. How powerful are graph neural networks? In *International Conference on Learning Representations*, 2019. URL <https://openreview.net/forum?id=ryGs6iA5Km>.
- Pinar Yanardag and SVN Vishwanathan. Deep graph kernels. In *Proceedings of the 21th ACM SIGKDD International Conference on Knowledge Discovery and Data Mining*, pages 1365–1374, 2015.
- Lingxiao Zhao and Leman Akoglu. Pairnorm: Tackling oversmoothing in gnns. In *International Conference on Learning Representations*, 2020. URL <https://openreview.net/forum?id=rkecl1rtwB>.